INTERNATIONAL ATOMIC ENERGY AGENCY

INDC(CCP)-422
Distr.: DN

I N D C INTERNATIONAL NUCLEAR DATA COMMITTEE

Fission Rate Determination in Delayed Neutron Emission Measurements with T(p,n) and D(d,n) Neutrons

V.M. Piksaikin, V.S. Shorin, R.G. Tertytchnyi

Institute of Physics and Power Engineering
State Scientific Centre of the Russian Federation
1 Bondarenko sq., Obninsk, Kaluga region, Russia 249020
Fax: +7-095-2302326
E-mail: piksa@ippe.rssi.ru

August 1999

Produced by the IAEA in Austria
August 1999

INDC(CCP)-422
Distr.: DN

Fission Rate Determination in Delayed Neutron Emission Measurements with T(p,n) and D(d,n) Neutrons

V.M. Piksaikin, V.S. Shorin, R.G. Tertytchnyi

Institute of Physics and Power Engineering
State Scientific Centre of the Russian Federation
1 Bondarenko sq., Obninsk, Kaluga region, Russia 249020
Fax: +7-095-2302326
E-mail: piksa@ippe.rssi.ru

Abstract

A method for accurate measurement of the fission rate in the samples irradiated by neutrons from the $T(p,n)^3He$ and $D(d,n)^3He$ reactions is described. The method is based on the measurements of the fission rate in two fission chambers placed in the vicinity of the sample and Monte-Carlo calculations of fission rates in the sample and in the chambers' fissionable layers. The Monte-Carlo calculations employ a neutron source procedure taking into account most of the factors influencing on the neutron spectra characteristics in conditions of a real experiment. An experimental procedure developed for testing the proposed method is discussed. The performance of the method is demonstrated by the results obtained in the measurements of the total delayed neutron yields from neutron induced fission of ^{237}Np and ^{235}U.

August 1999

Fission Rate Determination in Delayed Neutron Emission Measurements with T(p,n) and D(d,n) Neutrons

V.M. Piksaikin, V.S. Shorin, R.G. Tertytchnyi

Institute of Physics and Power Engineering
State Scientific Centre of the Russian Federation
1 Bondarenko sq., Obninsk, Kaluga region, Russia 249020
Fax: +7-095-2302326
E-mail: piksa@ippe.rssi.ru

Introduction

For better understanding of the neutron induced fission process of heavy nuclei as a whole and the mechanism of delayed neutrons (DN) emission in particular, it is interesting to know the DN emission properties and their dependences on an excitation energy of a fissionable nucleus. In this respect one of the least investigated values is the absolute DN yield $\nu_d(E_n)$ versus an incident neutron energy E_n. At the present time the detailed $\nu_d(E_n)$ data are available only for nuclei ^{233}U, ^{235}U, ^{238}U [1].

In experiments with a cyclic irradiation of researched sample the value $\nu_d(E_n)$ is determined by the relation [2]

$$N(E_n,t) = \varepsilon \cdot R(E_n) \cdot \nu_d(E_n) \cdot F(a_i,\lambda_i,t_k) \quad (1)$$

where $N(E_n,t)$ is the measured count rate of the DN detector at the time t after the end of irradiation (number of DN detector counts in a given time interval), ε is the neutron detector efficiency averaged on the DN energy spectrum; $F(a_i,\lambda_i,t_k)$ is the function depending on the values of relative DN yields a_i and decay constants λ_i, and also on the time parameters t_k (irradiation time and delayed neutron counting time, number of irradiation cycles etc.); $R(E_n)$ is the fission event rate. The value of ε is usually measured in a special experiment [3] whereas the value $R(E_n)$ characterizes experiment as a whole and depends on many factors (geometry of experiment, mass of a sample and its sizes and configuration, features of a neutron source etc.). Therefore from the methodical point of view the most complicated task is to determine the value of $R(E_n)$ at different energies of incident neutrons.

In the majority of experiments performed with thermal neutrons and with fission spectrum neutrons, the fission rate was determined via measuring a gamma and beta activity of fission products emerged in irradiation process of a sample [4,5]. However the application of such method to study the energy dependence $\nu_d(E_n)$ in a wide range of neutron energies causes difficulties because of absence of the reliable data on the energy dependence of fission product yields.

In the work [1] the fission rate was determined using the method of the absolute counting of fission fragments in the fission chamber when the fissile layer and the sample under investigation were exposed to almost equal neutron fluxes. For this purpose the sample was placed close enough to the fissile layer. Such experimental configuration did not allow to

transport the sample into a neutron detector after the irradiation, that essentially reduced DN count rate.

The purpose of the present work is to create a method of determination of fission event rate in a sample irradiated with quasimonoenergetic neutrons from the $T(p,n)^3He$ and $D(d,n)^3He$ reactions. The consideration is given for the case of the measurements of DN yields from neutron induced fission of ^{237}Np [2].

Fission rate in samples

In general the calculation of fission rate in the sample is a quite complicated problem [6] connected with solving the neutron transport kinetic equation taking into account neutron multiple scattering in a sample and construction materials of the experimental setup. It is necessary to account for a composite nonmonoenergetic spectrum of accelerator-based neutron source as well. In the general form the value of $R(E_n)$ can be presented as the functional of the following type:

$$R(E_n) = <\Sigma(E)\cdot\Lambda(\boldsymbol{r})\cdot \varphi(E,E_n,\boldsymbol{r})>_{E,\boldsymbol{r}} \qquad (2)$$

where $\Sigma(E)$ is the effective macroscopic fission cross-section for neutrons with energy E, $\Lambda(\boldsymbol{r})$ is the neutron path length in the sample in the direction of radius-vector $\boldsymbol{r}$ of the interaction point, $\varphi(E,E_n,\boldsymbol{r})$ is the neutron flux on the sample with average neutron energy E_n, the sign $<>_{E,\boldsymbol{r}}$ denotes the averaging over all coordinates $\boldsymbol{r}$ and neutron energies E. The value of $\varphi(E,E_n,\boldsymbol{r})$ is associated with a spectrum of accelerator-based neutron source φ_0 by the relation

$$\varphi(E,E_n,\boldsymbol{r})=\Phi_0(E_n)\cdot<\varphi_0(E',E_n\boldsymbol{\Omega})\cdot G(E'\rightarrow E,\boldsymbol{\Omega}\rightarrow\boldsymbol{r})>_{E',\boldsymbol{\Omega}}, \qquad (3)$$

where $\boldsymbol{\Omega}$ is the unit vector of an outgoing neutron direction, $\Phi_0(E_n)$ is the total neutron yield from an accelerator target, $G(E'\rightarrow E,\boldsymbol{\Omega}\rightarrow\boldsymbol{r})$ is the Green function (scattering indicatrix) of the system which is taking into account the features of neutrons transport for the given geometry of experiment (Fig. 1). Such geometry relates to the class of "tight (close) geometry", where the sample under study is located very close to a neutron source and consequently subtends a considerable solid angle relative to ion beam direction. Such geometry conditions and rather thick targets (0.6-2.0 mg/cm^2) used to obtain intensive neutron fluxes lead to the additional neutron energy spread due to the incident ion energy losses in the target material and to the angular kinematics broadening of neutron spectrum. These effects result in a noticeable width (up to 10-15% relative to E_n) and asymmetry of the spectrum φ_0. Another source of the neutron energy spread is connected with the secondary neutrons due to the processes of neutron slowing-down in the water layer (0.4 mm) used for the target cooling and due to neutron multiple scattering on the sample and on the experimental setup materials. These processes lead to occurrence of the low energy tail in the spectrum $\varphi(E,E_n,\boldsymbol{r})$. It is quite a problem to determine the spectrum φ_0 and especially the spectrum $\varphi(E,E_n,\boldsymbol{r})$ experimentally. Taking into account a high precision of the data on the neutrons emission reactions and on the neutron-matter interaction constants, more acceptable approach is to simulate it numerically. At the same time the normalization constant $\Phi_0(E_n)$ can be determined by the comparison of the calculated value with the count rates $R_i(E_n)$ of two monitor fission chambers (with fissile

layers made of the same material ^{237}Np, ***i*** is the chamber's number) located directly in front of and behind the researched sample in the same neutron flux. Use of two fission chambers for neutron flux monitoring essentially raises the reliability of the method because possible variations of a neutron field are taken into account in the course of the simulation.

By analogy to the expression (2) the fission rate in the fission chamber ***i*** can be written as

$$R_i(E_n)=\varepsilon^i\cdot\Phi_0(E_n)\cdot \boldsymbol{W_i}$$
$$\boldsymbol{W_i} =<\Sigma_i\cdot\Lambda_i\cdot\varphi_0{}^i\cdot\ G^i>\ , \qquad (4)$$

where ε^i is the efficiency of fission event registration for the fission chamber ***i.*** The procedure of the determination of the fission chamber efficiency ε is considered in the paper [7] in details. From Eq. (2-4) follows that the fission rate in the sample can be expressed as

$$R_s(E_n)=<R_i(E_n)\cdot\ \boldsymbol{W_i}^{-1}>_i\cdot\ \boldsymbol{W_s}\cdot\ (\varepsilon^i)^{-1}\ , \qquad (5)$$

where the index *s* relates to the sample; the sign $<\ >_i$ means the average value of the results obtained with two fission chambers. The equation (5) contains the measured values $R_i(E_n)$, the fission chambers' efficiencies ε^i, and the ratio of two functionals such as *W* which can be calculated by using the *MCNP* code [8] within the same scheme and with identical neutron interaction constants. Such procedure essentially decrease possible errors of the calculated value $R_s(E_n)$.

For *MCNP*-calculations it is essential to define the spectrum $\varphi_0(E',E_n\Omega)$ of the accelerator-based neutron source correctly. In the present work the spectrum φ_0 was simulated by the subroutine *"SOURCE"* [9] which can operate with a wide class of neutron sources (both solid and gas) based on the *(p, n)* and *(d, n)* - nuclear reactions. Its brief description is represented below.

Simulation of neutron source spectrum

Neutron spectrum $\varphi_0(E',\theta_n)$ where θ_n is the LS neutron angle relative to the incident ion beam direction, was calculated in correspondence with the diagram (Fig. 2) under the formula [10]:

$$\varphi_0(E',\theta_n)=const\cdot\iiiint dx\cdot d\Omega_p\,d\Omega\cdot dE_p\cdot G_1(\theta_p,x,E_0)\cdot G_2(E_p-\varepsilon_p(x,\theta_p,E_0))\cdot C(x)\cdot\ d\sigma_{pn}/d\Omega(E_p,\theta)$$
$$\cdot\ \delta(E'-\varepsilon_n(E_p,\theta))\cdot\ \delta(\theta_n-\chi(\theta_p,\theta)).$$

Here G_1 is the ion angle distribution function of incident ion energy E_0 and of the multiple scattering angle θ_p at the depth *x* from a target surface; $d\Omega_p$ and $d\Omega$ are the solid angle elements defined by the polar angles θ_p and θ respectively; G_2 is the energy loss distribution function of the ion energy E_p at the depth *x*; $\varepsilon_p(x,\theta_p,E_0)$ is the mean ion energy; $C(x)$ is the concentration profile of the target material; $d\sigma/d\Omega$ is the neutron production differential cross section; δ is the character of the Dirac delta function; ε_n is the neutron energy function kinematically connected with the ion energy E_p and with neutron emission angle θ; χ is the function coupling the angles θ_n, θ_p and θ. The indexes *p* and *n* denote a projectile and escaping neutron respectively.

The following approximations were included:

A. The function G_1 was supposed to have a form $G_1(y)=exp(-y)$, where $y=\theta_1^2(x)/\langle\theta_1^2\rangle(x)$ and $\langle\theta_1^2\rangle(x)$ is the mean square of multiple scattering angle of ions in the target matter, i.e. the small scattering angles approximation was used.

B. The function G_2 was supposed to be a Gaussian, though it is known that for small energy losses it is described by the Vavilov distribution.

C. The targets of a multielement composition with the number of components not more than 6 are considered.

D. The multilayer targets with the number of layers not more than 6 are considered; inside each layer the function $C(x)$ for the given component is considered as a constant value. This approximation allows to operate with both solid and gas targets.

E. The case of normal incidence of a wide ion beam uniformly distributed in the circle of radius R_d on the target surface is considered. The centre of the beam can be biased relative to an axis of a cylindrical target.

The calculation of the spectrum of primary neutrons requires a solution of the ion stopping problem for the multilayer target of multicomponent composition. This problem was reduced to the numerical solving of the system of the first order differential equations for the first four moments of the ion energy distribution function in a target matter. The first two moments, namely the values $\varepsilon_p(x,\theta_p,E_0)$ and energy straggling $s_p(x,E_0)$ were used for simulating the function G_2, second two - the coefficient of skewness and kurtosis - were used to estimate the accuracy of the approach. As a part of the solution the angular values $\langle\theta_1^2\rangle(x)$ were calculated. All calculations were based on the ions stopping data dE/dx in matter obtained with the help of the well-known code *TRIM* (version 91.14) [11]. For given energy E_p the dE/dx values were calculated using the cubic spline - interpolation. For multielement targets (compounds) the Bragg rule was used. To calculate the functions $\varepsilon_n(E_p,\theta)$ the relativistic kinematic formulae for two-particle nuclear reactions [12] and the atomic masses table Audi-93 [13] were used. The code operates with the following neutron production reactions: T(p,n), D(d,n), T(d,n), ^{7}Li(p,n)^{7}Be and ^{7}Li(p,n)^{7}Be* (and the inverse to them). The data on the neutron production cross-section in the center-of-mass system (CM) were taken from [14] and appropriate extrapolation was used near threshold range for *(p,n)* – reactions.

The code is written in *"Fortran–77"* for compiler *f77L-EM/32* version 5.01. Its main part is the subroutine *nsource (EN, OM, X, Y, Z, WGT)* which generates random variables, namely *EN* - the neutron energy in MeV, *OM (1)*, *OM (2)*, *OM (3)* - the direction cosines of the unit vector defining the neutron direction relative to axes *OX*, *OY* and *OZ* respectively; *X*, *Y*, *Z*-the coordinates of neutron birth point (coordinate *Z* is chosen along the incident beam axis); *WGT* -the neutron weight (number of neutrons per 1 μKl). At the first call of the program the initial data are entered. Then the stopping problem is solved. As a result the text file containing the mean ion energy $E_p(t)$ (MeV), the straggling $s_p(t,E_0)$ (MeV) and $\langle\theta_1^2\rangle(t)$ on the depth t (mg/cm^2) in the tabulated form is produced. After the sampling of coordinates *(X, Y)* of the interaction point in the circle of radius R_d and *Z*-coordinate of the neutron birth point, the values $E_p(z)$, $s_p(z)$, $\langle\theta_1^2\rangle(z)$ are calculated by a linear interpolation. Further the

appropriate random values are calculated using the normal numbers generator and random numbers generator for an exponential distribution. Then the outgoing neutron direction angle *(cos(θ), sin(θ))* in the CM system for the two-particle reaction is sampled uniformly in the range from -1 to +1. The statistical weight *WGT* proportional to the differential reaction cross-section $d\sigma(E_{p,d},\theta)/d\Omega$ is assigned to the neutron birth event. Further outgoing direction angles of neutrons are transformed from the CM system to the LS system, the outgoing neutron energy *EN* and the *OM*-values are calculated (the presence of two groups of outgoing neutrons for threshold reactions is taken into account). The results of the *MCNP*-calculations of $\varphi_0(E',E_n\boldsymbol{\Omega})$ and $\varphi(E,E_n,\boldsymbol{r})$ spectra are shown below.

Results

In Figures 3 and 4 the calculated neutron spectra $\varphi(E,E_n,\boldsymbol{r})$ for T(p,n)^{3}He - neutrons interacting with the ^{237}Np sample and ^{237}Np fissile layer in the fission chamber are shown. One can see the effects of the neutron flux attenuation and multiple scattering on the constructional materials of the experimental setup. The calculations were carried out for layout of the sample and the fission chambers relative to the neutron source shown in Fig. 1. The layers of the fission chambers were made of dioxide of neptunium. The thickness of fissile layers was 100 μg/cm^2, diameter - 2 cm. The sample was made of dioxide of neptunium and represents the cylinder 0.29 cm diameter and 1.5 cm height placed in the container of stainless steel.

As it is shown in Figs 3 and 4 the neutron distributions $\varphi\langle E,E_n,\boldsymbol{r}\rangle_{\boldsymbol{r}}$ averaged over the volumes of the sample and the fissile layer for the same incident ions energy (E_0 =1.318, 1.550, 1.777, 1.974 MeV) have essentially different shapes, dispersions and asymmetry. This can be seen also from the Table 1 where three first moments of the neutron spectra related to the sample are presented. The low energy "tail" in the neutron spectrum on the sample due to the neutron multiple scattering effects can be seen. It is important to take into account this component in the measurements with non-threshold fissile isotopes. Besides that in both cases the shape of distributions has a strong energy dependence and their mean neutron energies are rather different. Taking into consideration the energy dependence of ^{237}Np fission cross-section, one can expect a considerable energy dependence of the ($\boldsymbol{W}_i^{-1}\,\boldsymbol{W}_s$) ratio value of the fission rates in the sample and fission chamber in the vicinity of the fission threshold for the case of "tight geometry".

The test of the method (to estimate the $R_s(E_n)$ value properly) was carried out by measuring the count rate $R_i(E_n)$ in the fission chambers placed at different distances from the neutron target and by comparing the results with calculated values $\boldsymbol{W}_i$. The results of the comparison are shown in Fig. 5. The light circles are the experimental data $R_i(E_n)$ obtained using the fission chamber placed between the neutron source and the sample. The black circles show the data for the fission chamber located behind the sample. The black squares connected by solid curve show the calculated values $\boldsymbol{W}_i$. In the insert the ratio of the experimental fission rate to the calculated one is presented. As one can see from the figure the discrepancy of the experimental values of the fission rates and the calculated ones does not exceed 1.5% in a wide range of distances from the neutron source to the fission chamber. Therefore the accuracy of the determination of the $R_s(E_n)$ values based on the calculation of the functionals $\boldsymbol{W}_i$ and $\boldsymbol{W}_s$ for actual samples should not exceed the quoted value.

In Fig. 6 the results of calculations of the values ($W_i \cdot W_s^{-1}$) for the ^{237}Np sample obtained for two cases of neutron flux monitoring (by one and two fission chambers) are presented. The energy dependence of this value in the range of neutron energies for T(p, n)^{3}He - reaction is defined by the difference in the average neutron energies in the sample and in the fission chamber. In the case of the D(d,n)^{3}He neutrons the increase of the ($W_i \cdot W_s^{-1}$) value with neutron energy is determined by the kinematics of the neutron production reaction. The calculations show that the neutron transport effects does not lead to considerable changes in the energy dependence of the fission rate ratios, while the shifts of the absolute value of the ratio are noticible (about 10%). It can be seen from Fig. 6 that for the case of "tight geometry" the fission rates ratio is close to a constant in the range of the average neutron energies 1-3 MeV. Such behaviour essentially simplifies the data analysis on the energy dependence $\nu_d(E_n)$ in the range of energies where there is a transition from one neutron source to the other and raises the reliability of the normalization method.

In Fig. 6 (black circles) the calculation results of the value ($W_i \cdot W_s^{-1}$) are shown for the case when two fission chambers were used in the experiment for neutron flux monitoring. The data are given for the fission chamber being placed behind the sample. The energy dependence of the ratio is flatter in this case. This "two fission chamber" configuration was used for measuring the absolute yield of delayed neutrons.

The method of the fission rate determination in the sample presented here was used to study the energy dependence of DN total yield from fission of ^{235}U and ^{237}Np in the energy range 0.4-5 MeV. The results are shown in Fig. 7. These data are obtained in two experiments (with one and two fission chambers). In the case of ^{235}U a good agreement of our results with the data [1] is observed. In the case of ^{237}Np the data on the energy dependence of DN total yield are obtained for the first time and show considerable dependence of ν_d on the incident neutron energy.

REFERENCES

[1] M.S. Krick, A.E. Evans, Nucl. Sci. Eng., 1972, Vol. 47, p. 311.

[2] V.M. Piksaikin, Yu.F. Balakshev, S.G. Isaev, L.E. Kazakov, B.D. Kuzminov, N.N. Semenova, A.I. Sergachev, M.Z. Tarasko, In: Proc. Int. Conf. Nucl. Data for Sci. and Technol., Trieste (19-24 May 1997), Conference Proceedings edited for Italian Physical Society, No. 59, 1998, p. 485.

[3] V.M. Piksaikin, S.G. Isaev, V.V. Korobeinikov, G.G. Korobeinikov, G.G. Korolev, N.N. Semenova, A.I. Sergachev, In: Proc. Int. Conf. Nucl. Data for Sci. and Technol., Trieste (19-24 May 1997), Conference Proceedings edited for Italian Physical Society, No. 59, 1998, p. 646.

[4] C.B. Besant, P.J. Challen, M.H. McTeggart, P. Tavoularidis, J.G. Williams, Journ. Br. Nucl. Energy Soc., Vol. 16, 1977, p. 161.

[5] G.R. Keepin, Physics of Nuclear Kinetics, Addison Wesley Publishing Co., Reading, Massachusetts, 1965.

[6] K.H. Bekurts, K. Wirtz, Neutron Physics, Springer-Verlag, Berlin, Göttingen, Heidelberg, New York, 1964, Ch. 11.

[7] J.A. Grundl, D.M. Gilliam, N.D. Dudey, R.J. Popek, Nucl. Techn., 1975, Vol. 25, p. 237.

[8] MCNP, A General Monte Carlo N-Particle Transport Code, Version 4A, J.F. Briesmeister (Ed.), Report LA-12625-M (1993).

[9] R.G. Tertytchnyi, V.S. Shorin, Preprint IPPE-2743, 1998 (in Russian).

[10] S.V. Tikhonov, V.S. Shorin, VANT (Voprosy Atomnoy Nauki i Tekhniki: Ser. Yadernye Konstanty, 1987, No. 3, p. 39 (in Russian).

[11] J.F. Ziegler, J.P. Biersack, U. Littmark, The Stopping and Range of Ions in Solids, Vol. 1 (Pergamon Press, N.Y.), 1985.

[12] J. Monahan, Fast Neutron Physics, J.B. Marion, J.L. Fowler (Eds), Interscience Publishers Inc., N.Y., Interscience Publishers Ltd., London, 1963, Vol. 1.

[13] G. Audi, A.H. Wapstra, Nucl. Phys., A565, 1993, p. 1.

[14] M. Drosg, O. Schwerer, Handbook on Nuclear Activation Data, IAEA, Vienna, 1987, Tech. Rep. 273, p. 83, M. Drosg, Computer-Code, Drosg-96 (15 December 1996), Documentation Series (O. Schwerer, Ed.), IAEA-NDS-87, Vienna, 1997.

[15] P.F. Rose (Ed.), "ENDF/B-VI Summary Documentation", report BNL-NCS-17541 (ENDF-201), (Brookhaven National Laboratory 1991). Data Library ENDF/B-VI, update 1998, by the U.S. National Nuclear Data Center on behalf of the Cross-Section Evaluation Working Group.

[16] C.F. Masters, M.M. Thorpe, D.B. Smith, Nucl. Sci. Eng., 1969, Vol. 36, p. 202.

[17] H.K. Saleh, T.H. Parish, et al., Nucl. Sci. Eng., 1997, Vol. 125, p. 51.

[18] A.N. Gudkov, et al., At. Energ., Vol. 66, No. 2, p. 100, 1989 (in Russian).

[19] G. Benedetti, A. Cesana, et al., Nucl. Sci. Eng., 1982, Vol. 80, p. 379.

[20] R.W. Waldo, R.A. Karam, Trans. Am. Nucl., 1981, Vol. 39, p. 879.

[21] R.J. Tuttle, In: Proc. of the Consultants' Meeting on delayed Neutron Properties, Vienna, 26-30 March 1979, IAEA, INDC(NDS)-107/G, p. 29.

[22] W. Charton, T. Parish, S. Raman, N. Shinohara, M. Andoch, In: Proc. Int. Conf. Nucl. Data for Sci. and Technol., Trieste (19-24 May 1997), Conference Proceedings edited for Italian Physical Society, No. 59, 1998, p. 491.

[23] D.J. Loaiza, G. Brunson, R. Sanchez, K. Butterfield, Nucl. Sci. and Eng., 1998, Vol. 128, p. 270.

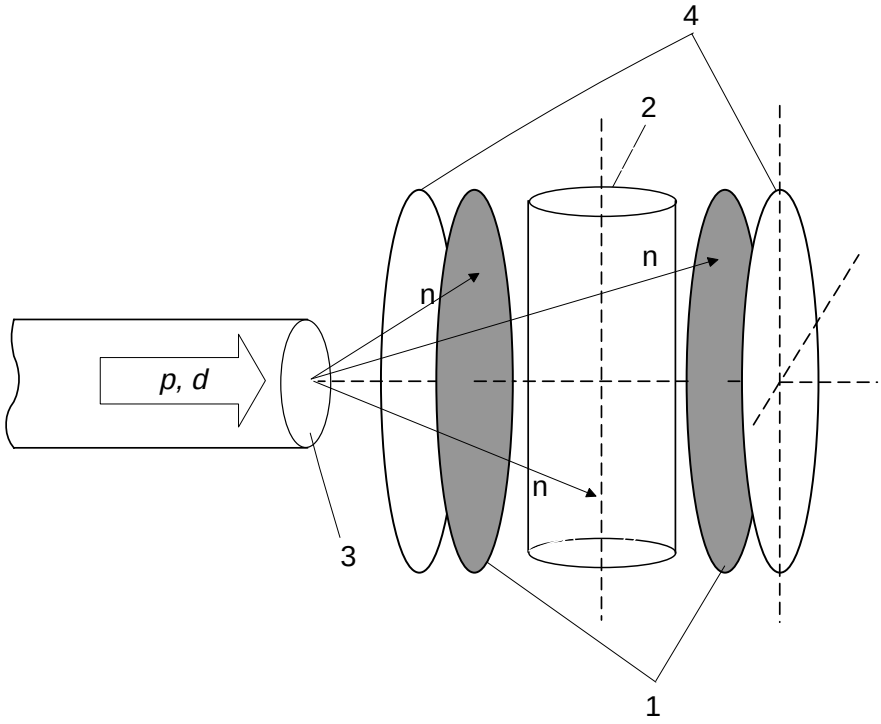

Fig. 1. The scheme of the experiment.
1 - ^{237}Np fissile layer, 2 - ^{237}Np sample, 3 - neutron target, 4 - fission chambers.

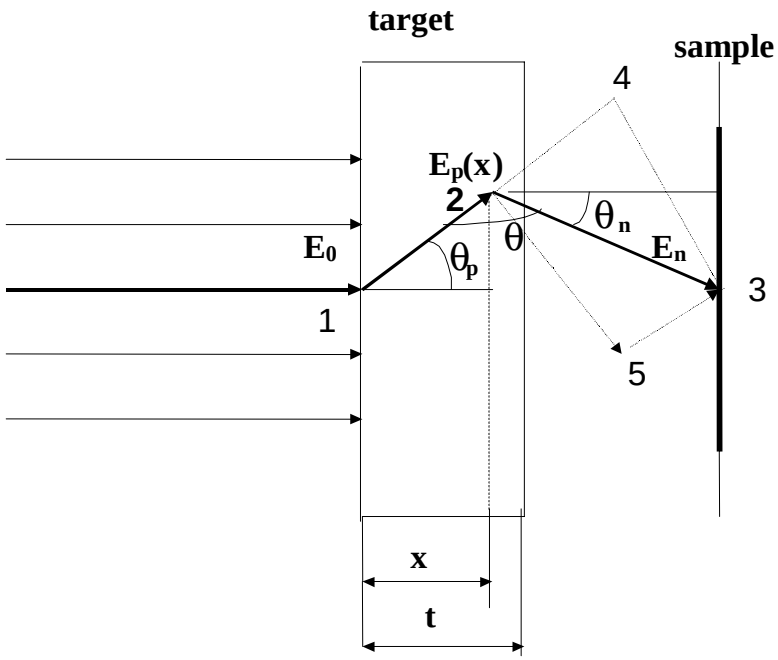

Fig. 2. The diagram for calculation of the neutron spectrum $\varphi_0(E_n,\theta_n)$. E_n and E_0 - the energies of outgoing neutron and incident ion respectively, $E_p(x)$ - the ion energy at the depth x, θ_p - the angle of multiple scattering, θ - the outgoing neutron direction angle relative to the direction of the ion at the point of interaction, θ_n - the outgoing neutron direction angle relative to the direction of the incident ion at the point x=0. 1 - the entry point of the ion in a target, 2 - the point of interaction, 3 - the point of neutron absorption in the sample, 4, 5 - the points of neutron scattering outside of a target.

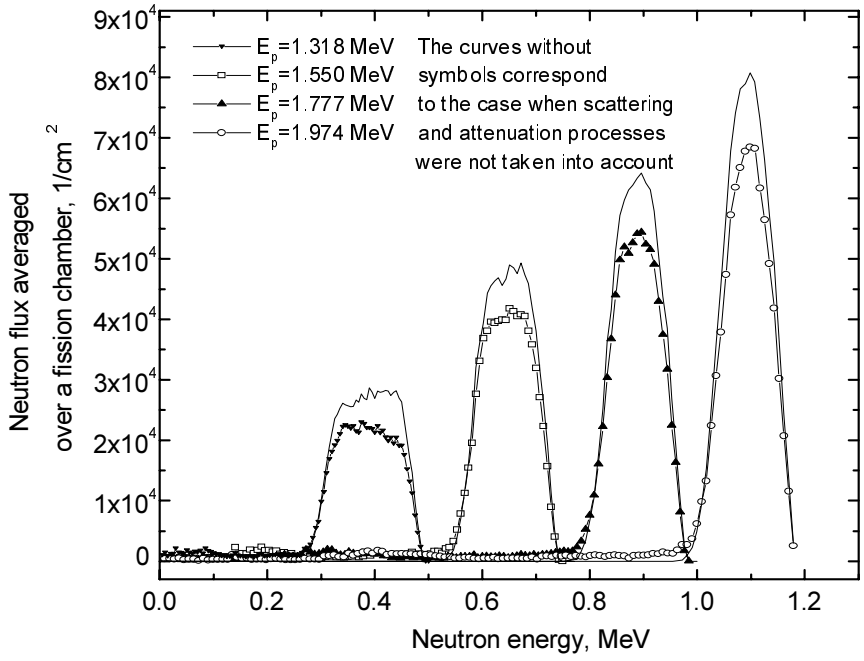

Fig. 3. Neutron energy distribution averaged over fissile layer of a fission chamber $\langle\varphi(E,E_n,\mathbf{r})\rangle_r$. *The upper curves are obtained for the case when only kinematic effects of a broadening of neutron spectra were taken into consideration. The lower curves are obtained for the case when all effects influencing on the shape of the neutron spectrum are taken into account.*
(Explanation see in Fig. 2.).

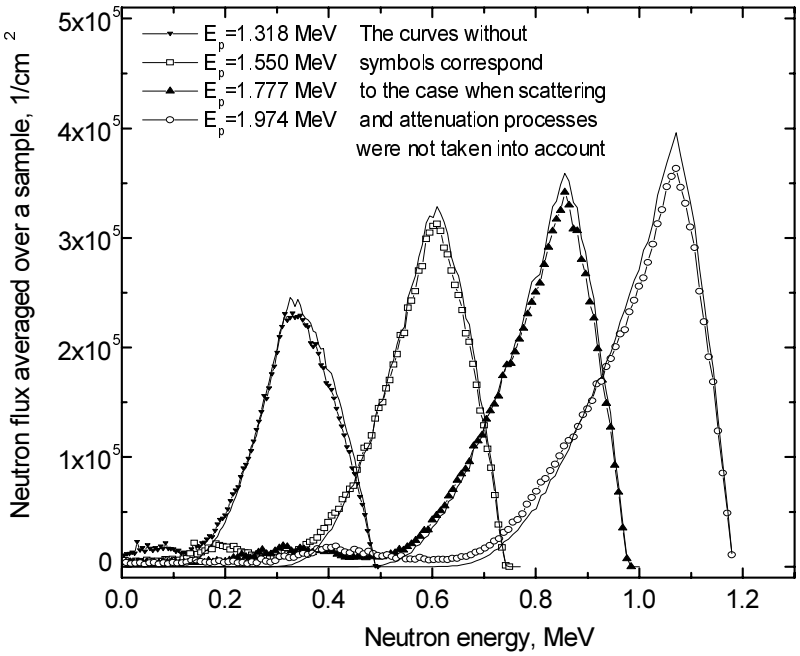

Fig. 4. The neutron energy distribution averaged over sample $\langle\varphi(E,E_n,\mathbf{r})\rangle_r$.

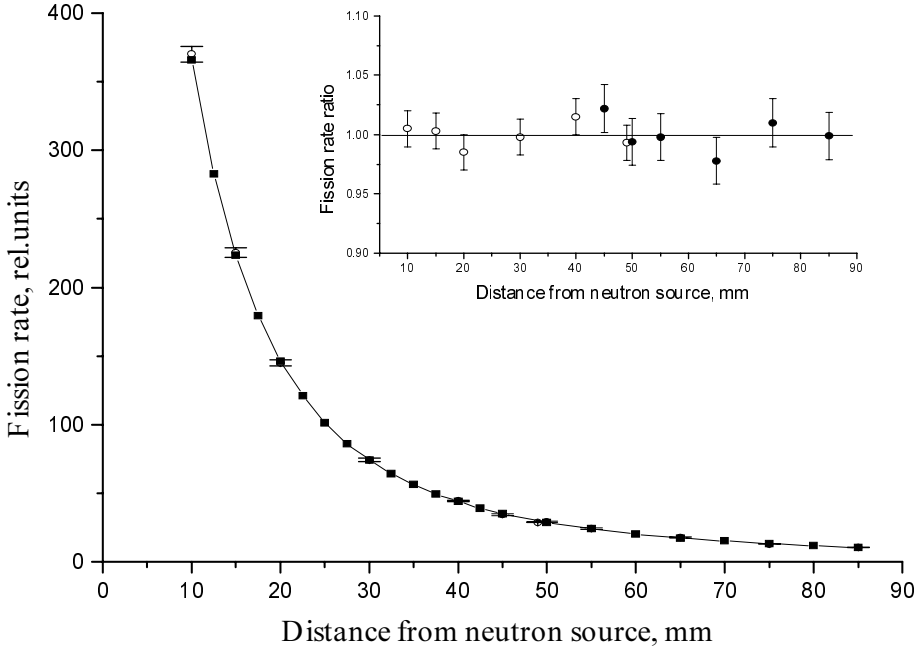

Fig. 5. Comparison of fission rates in the fission chambers at different distances from a neutron source T(p, n) obtained by measuring R_i (E_n) and on the basis of $\boldsymbol{W}_i$ calculations. The energy of primary protons is 1.974 MeV. The data are explained in the text.

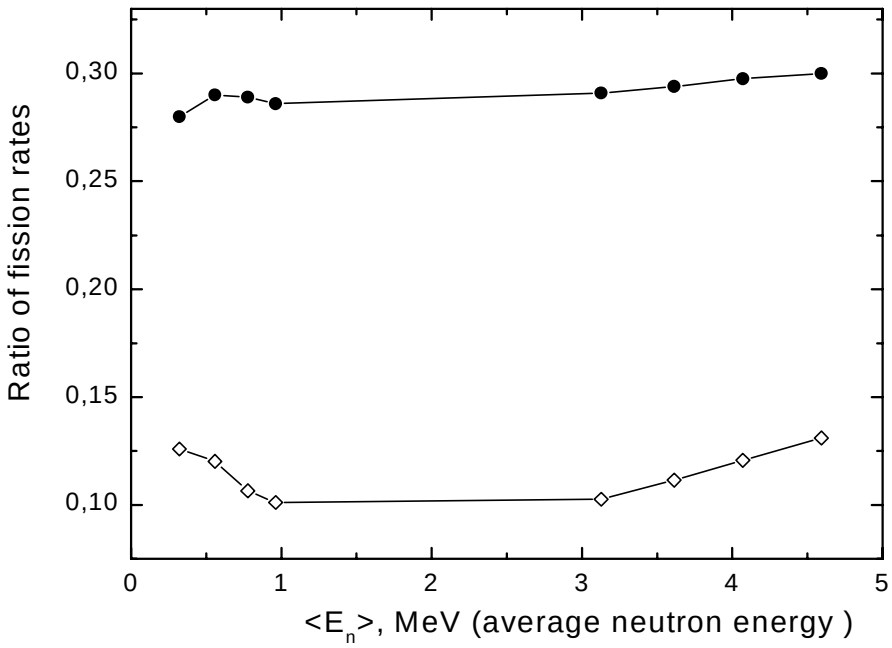

Fig. 6. The ratio of fission rates in a layer of fission chamber and ^{237}Np sample $\boldsymbol{W}_i \cdot \boldsymbol{W}_s^{-1}$. Open circles are related to "one fission chamber" geometry. Black circles are related to "two fission chambers" geometry. The points are connected by straight lines for visualization.
The dependence in the energy range 1-3 MeV was not calculated.

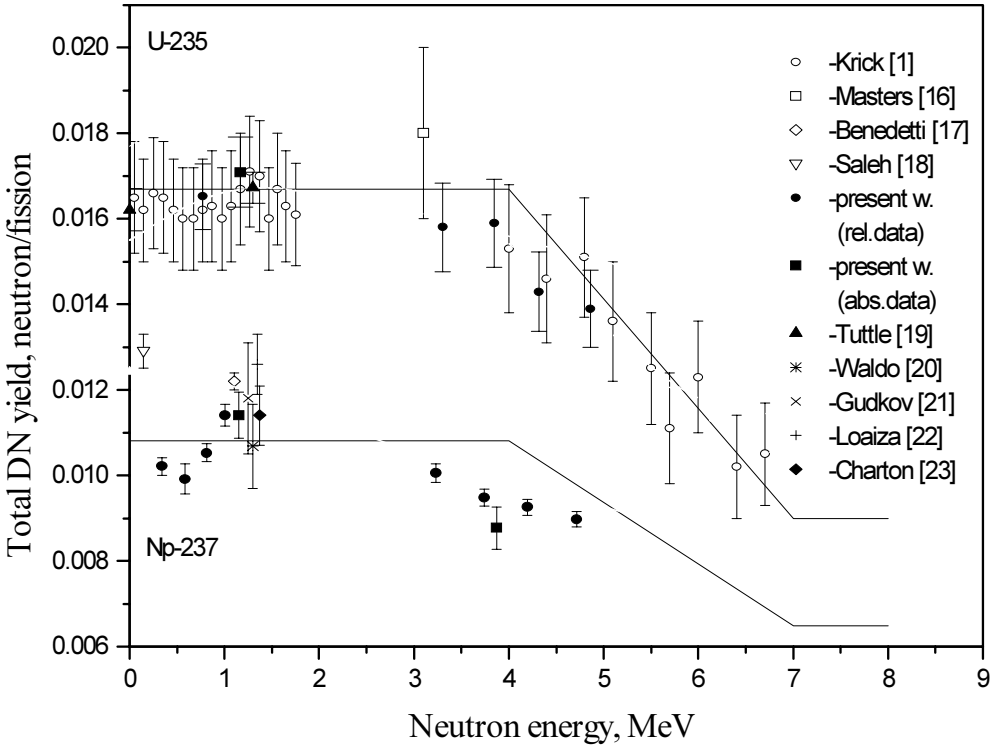

Fig. 7. The energy dependence of the DN total yield from neutron induced fission of ^{235}U and ^{237}Np.
Solid lines - [15]. Data from [17, 20, 21, 22, 23] are related to fast neutron spectra and their abscises are shown roughly.

TABLE 1. THE FIRST THREE MOMENTS OF THE NEUTRON SPECTRA ASSOCIATED WITH T(p,n)^{3}He - NEUTRON SOURCE FOR THE Ti-T TARGET THICKNESS 1.0 g/cm^2

Fission chamber				Sample		
Proton energy, MeV	Average neutron energy, MeV	Neutron energy spread, MeV	skewness	Average neutron energy, MeV	Neutron energy spread, MeV	skewness
1.318	0.366[a)] 0.390[b)]	0.088 0.050	-1.851 -0.088	0.324 0.340	0.090 0.070	-0.964 -0.255
1.550	0.616 0.651	0.119 0.043	-2.834 -0.080	0.561 0.586	0.121 0.077	-1.721 -0.480
1.777	0.850 0.892	0.147 0.040	-3.313 -0.089	0.780 0.814	0.151 0.089	-2.065 -0.627
1.974	1.048 1.096	0.175 0.039	-3.532 -0.134	0.967 1.008	0.180 0.099	-2.270 -0.073

a) The fist row contains the results of calculations including all the neutron transport effects.
b) The second row is related to the calculations taking into account of the kinematics of the neutron production reaction and target thickness only.

Nuclear Data Section
International Atomic Energy Agency
P.O. Box 100
A-1400 Vienna
Austria

e-mail: services@iaeand.iaea.or.at
fax: (+43-1) 26007
cable: INATOM VIENNA
telex: 1-12645
telephone: (+43-1) 2600-21710

Online: TELNET or FTP: iaeand.iaea.or.at
username: IAEANDS for interactive Nuclear Data Information System
usernames: ANONYMOUS for FTP file transfer;
FENDL2 for FTP file transfer of FENDL-2.0;
RIPL for FTP file transfer of RIPL;
NDSONL for FTP access to files sent to NDIS "open" area.
Web: http://www-nds.iaea.or.at